

LIDAR MEASUREMENTS OF SEA SURFACE WAVES

K. I. Voliak and M. V. Solntsev
General Physics Institute of the USSR Ac. Sci.
38 Vavilov st., 117942 Moscow, USSR, Commission VII

ABSTRACT. A lidar method is developed to measure the sea wave spectrum and other sea characteristics by using a narrow amplitude-modulated beam. Some techniques are suggested for determining the slope and curvature variance from a backscattered (reflected) power. The model field experiment was carried out at an oceanographic platform. The experimental data demonstrate that the introduced method is highly effective.

1. INTRODUCTION. To study spatial-time structures of sea waves is urgent for solution of various scientific and applied problems arising in the field of oceanic physics. Remote sensing methods seem to be very appropriate for this purpose. The most highly developed technique of oceanic remote sensing is associated with the use of air-space imaging radars. Now in radiooceanography the so-called synthetic aperture radars [1], recording the coherent backscatter from the sea, or the noncoherent side-looking radars [2] enjoy great favor.

Since the early 1970s laser methods of sea probing have been also developing. They are superior to radiooceanography in several respects. First, lidars can provide higher spatial-time resolution, which is suitable for measuring small-scale waves. For instance, a sharp-focused laser beam permits us to measure waves of a horizontal scale up to 1 mm, while the microwave radar resolution is limited just to several meters. The duration of a radar pulse is typically from 10^{-7} to 10^{-9} s [3]; accordingly, the spatial resolution is 0.15-15 m. In the optical range one can produce pulses as short as $5 \cdot 10^{-13}$ s [4] enabling a resolution of 0.08 mm to be obtained. We observe the principal difference between radar and lidar probings in the reflection of signals by the sea. The radar wave length exceeds often those of the capillary waves, and, therefore, various diffraction effects are of importance here. Meanwhile the laser wave length is considerably shorter than any surface one, and the mechanism of laser reflection is reasonably explained in terms of geometric optics. This aspect gives rise to much simpler relations between the statistics of the lidar return and that of the sea surface, compared to radars. One of the important parameters of the lidar return is its average power. As shown theoretically [5], [6], lidar measurement of an average backscattered power at different incidence angles establishes variances β_x and β_y of the downwind and crosswind components of the surface slope.

Presently there are two principal ways of oceanic lidar remote sensing, namely, pulse ranging and phase profilometry. The former [7] involves determination of the time delay between sounding and reflected pulses as well as analysis of their shapes and durations. Depending on the experimental facilities and position (for example, on the beam divergence and vertical or slant incidence), we can estimate the significant wave height, the slope probability density, or measure roughly the sea

surface profile. Laser measurement of the profile can be also carried out with airborne phase altimeters. Continuous flight altitude measurements permit reconstruction of the surface profile along the flight ground line [8].

An analysis of the state of the art in these methods [9] reveals that the two techniques are effectively applicable to investigation of sea waves as long as 10m and more. But in many field experiments it is important to study both large-scale and comparatively short waves. A good example of this situation is the interaction between internal and surface waves, where most changes are observed just in the short surface wave spectrum. Further development of laser investigations of cm and dm sea waves requires a finer spatial resolution. In the field of pulse ranging one can decrease the sounding pulse duration. The use of subnanosecond laser techniques calls for faster and, hence, more sophisticated receivers.

2. NARROW-BEAM LIDAR RETURN FROM THE SEA SURFACE. Let a laser beam of an intensity $I(r, \theta)$, where r is the distance from the beam axis and θ is the azimuthal angle, be normally incident upon the sea surface. In the horizontal plane at above-surface elevation H , there is placed a receiving aperture D (Fig.1). The distance between the axes of the beam and the aperture equals l . The characteristic diameter of a sounding beam is equal to d . Then introduce the coordinates (x, y, z) with their origin at the receiver axis. The coordinates x, y lie in the horizontal plane of an undisturbed surface, and z is directed upwards. Any point of the surface is defined by its elevation $\xi(x, y)$ and the slope vector

$$\vec{\rho}(x, y) = (\xi_x = d\xi/dx, \xi_y = d\xi/dy) . \quad (1)$$

The momenta of the directional surface spectrum $E(k_1, k_2)$ can be written in the form :

$$m_{ij} = \iint_{-\infty}^{\infty} E(k_1, k_2) k_1^i k_2^j dk_1 dk_2, \quad i, j = 0, 1, 2, \dots, \quad (2)$$

where $\vec{k} = (k_1, k_2)$ is the wavevector of surface random disturbance.

To evaluate the statistics of the return, it is necessary to assume the following: (i) the surface slopes are obviously gentle, $m_{20}, m_{02} \ll 1$; (ii) the altitude is great, $H \gg \langle \xi^2 \rangle^{1/2}$; (iii) the sea return is homogeneous within the beam spot, $d/H \ll m_{20}, m_{02}$; (iv) the transmitter and the receiver are nearly coaxial $l/H \ll m_{20}, m_{02}$; (v) the beam is narrow, $nS \ll 1$, where n is the density of specular points at surface slopes $\xi_x = \xi_y = 0$, and S stands for the spot square; and (vi) the surface is illuminated from the 'far' range, $D \langle |R| \rangle / H \ll n^{-1/2}$, where $\langle |R| \rangle$ is the average modulus of the radius of surface curvature. Under all these conditions the lidar return from the sea surface is provided by the specular points within the lidar spot. The power returned from a single specular point is

$$P_s = 0.0625\pi |\Omega|^{-1} (D/H)^2 \rho_0 I(r, \theta). \quad (3)$$

Here $\rho_0 \approx 0.02$ is the sea reflectivity at the normal incidence,

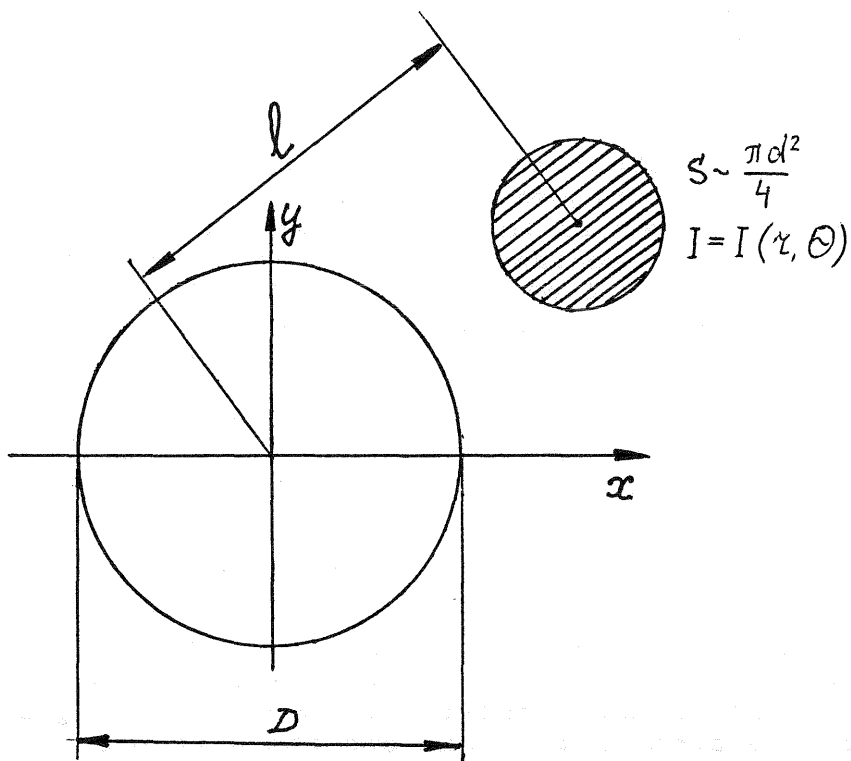


Fig.† Horizontal cross-section of the probing geometry.

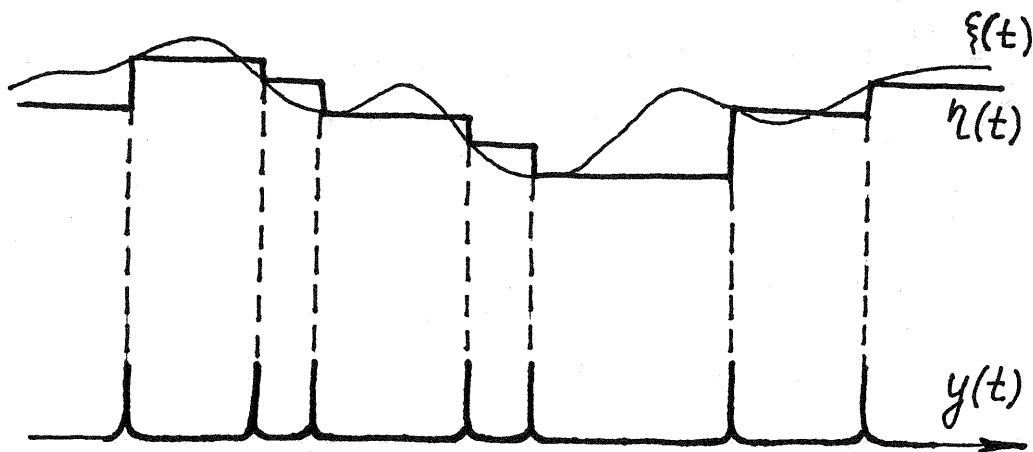


Fig.2 Discretization of the process $\xi(t)$ by a random pulse sequence $y(t)$.

Ω is the total curvature at the specular point. Let us normalize the point return as

$$P_s^o = \begin{cases} 1, & \text{if the specular point is placed inside the beam spot,} \\ 0, & \text{if it is outside the spot.} \end{cases}$$

Assuming that the sea surface is a random Gaussian field, one can obtain some statistical quantities: the average power

$$\langle P_s \rangle = \alpha / \delta ; \quad (4)$$

the power variance

$$\langle P_s^2 \rangle = \frac{\alpha^2 \langle |\Omega^{-1}| \rangle}{P_o^2 \delta} \iint_{o \ o}^{2\pi} I^2(r, \theta) r \ dr \ d\theta ; \quad (5)$$

and the average normalized return

$$\langle P_s^o \rangle = \langle |\Omega| \rangle S / \delta = nS. \quad (6)$$

Here $\alpha = 0,0625\pi D^2 H^{-2} \rho_o P_o$, P_o is the radiated power, $\delta = 2\pi \Delta_2^{1/2}$, and $\Delta_2 = (\beta_x \beta_y)^2 = m_{20} m_{02} - m_{11}^2$ is the surface invariant, which depends on the wave steepness and divergence.

Thus, the measurements of $\langle P_s \rangle$, $\langle P_s^2 \rangle$, $\langle P_s^o \rangle$ make feasible to determine the sea cross-section σ , the invariant Δ_2 , and the mean moduli of the curvature and of its reciprocal:

$$\sigma = (\langle P_s \rangle / P_o) 4\pi^{-1} (H/D)^2, \quad \Delta_2^{1/2} = \alpha / 2\pi P_s, \quad (7), (8).$$

$$\langle |\Omega| \rangle = \frac{\alpha \langle P_s^o \rangle}{\langle P_s \rangle}, \quad \langle |\Omega^{-1}| \rangle = \frac{\langle P_s^2 \rangle P_o^2}{\alpha \langle P_s \rangle} \left(\iint_{o \ o}^{\infty 2\pi} I^2(r, \theta) r \ dr \ d\theta \right)^{-1}, \quad (9), (10)$$

respectively.

3. PHASE PROFILOMETRY WITH A NARROW BEAM. In the case of phase profilometry, the laser beam is amplitude-modulated with some frequency f . The return is formed by specular points mentioned above. To monitor the profile continuously, the lidar surface spot should be widened, thereby degenerating spatial resolution and averaging surface elevation over the spot. Oceanographers are primarily concerned in the sea spectrum or other statistical quantities rather than in isolated sea elevation records. The problem is, therefore, to reconstruct the statistics of an unknown random sea from an experimental discrete sample corresponding to the specular points.

Let $\xi(t)$ be a stationary random function of the surface elevation in time (or in space). The discretization of $\xi(t)$ (Cf. Fig. 2) by a random sequence $y(t)$ produces a new random

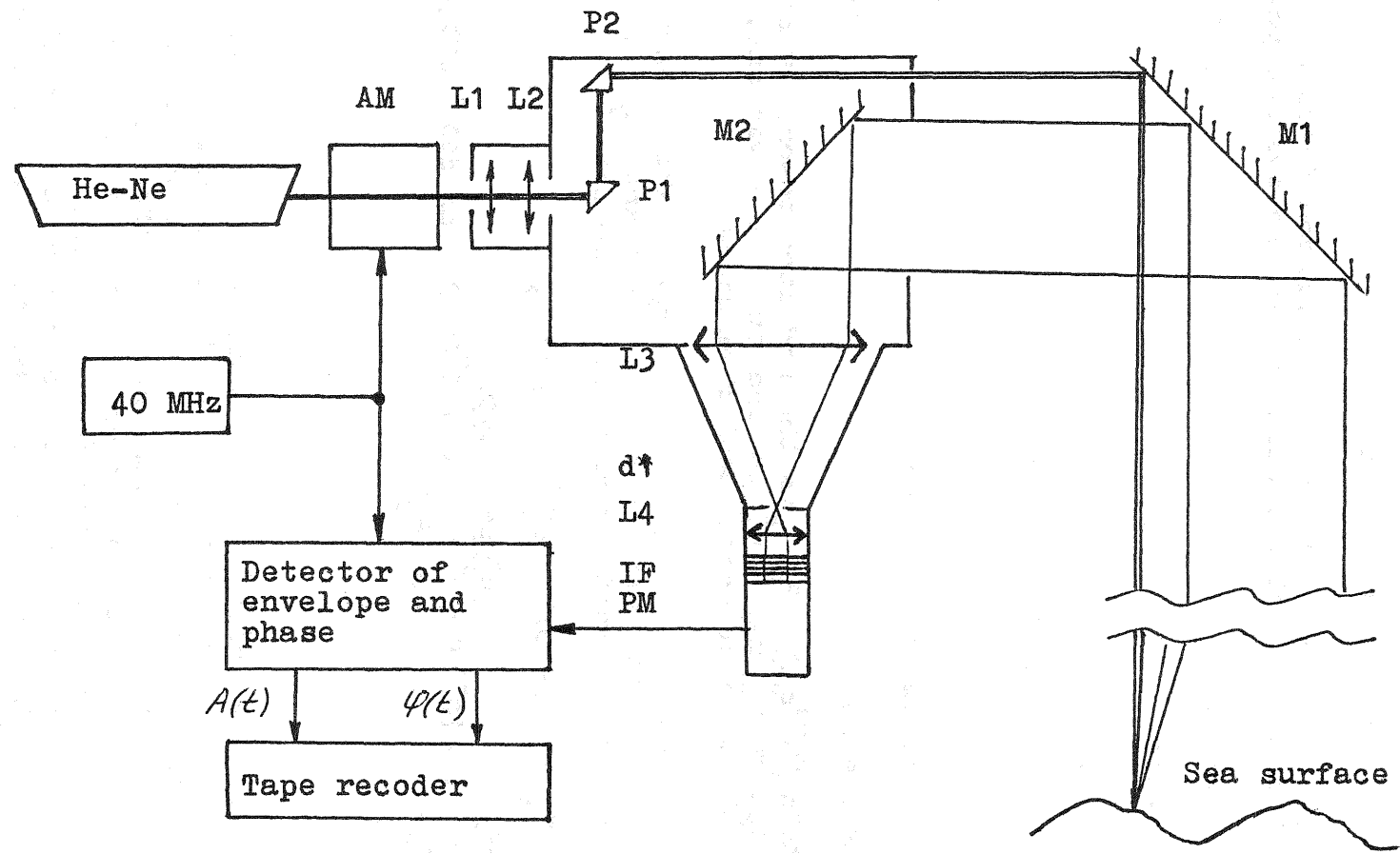


Fig.3 Experimental set-up.

$\eta(t)$. If $\eta(t)$ is of the Poisson distribution with a mean pulse period τ_0 , the spectrum $S_2(\omega)$ of $\eta(t)$ depends on the spectrum $S_1(\omega)$ of $\xi(t)$ as [10]:

$$S_2(\omega) = \frac{1}{1 + \omega^2 \tau^2} \left[S_1(\omega) + S_0 \right], \quad S_0 = \frac{2\tau^3}{\pi} \int_0^{\infty} \frac{(\omega')^2 S_1(\omega')}{1 + (\omega')^2 \tau^2} d\omega'. \quad (11)$$

It is evident from (11) that the discretization of a random process by a pulse Poisson sequence is equivalent to incorporation of a high-pass filter of a cut-off frequency $\omega_0 = \tau_0^{-1}$, which is connected in parallel with the source of 'white' noise of the spectrum S .

For an initially limited sea spectrum, where $S_1(\omega) = 0$ at $\omega > \omega_m$, we reconstruct $S_1(\omega)$ by the following: (i) $S_2(\omega_1)$ is evaluated at $\omega_1 > \omega_m$; (ii) the 'white' noise spectrum $S_0 = S_2(\omega_1)(1 + \omega_1^2 \tau_0^2)$ is found; and (iii) the initial spectrum $S_1(\omega) = S_2(\omega)(1 + \omega^2 \tau_0^2) - S_0$ is reconstructed. When probing is carried out from a stable platform, we can show that the sea specular glitter is described rather well by the Poisson statistics, that allows us to apply the suggested algorithm for reconstructing the sea spectrum.

4. EXPERIMENTAL SYSTEM AND SITE. To study the statistics of the laser return from the sea surface, we have designed a lidar shown schematically in Fig.3. The source was a 15mw CW He-Ne red (633nm) laser LG-79/1. The sounding beam was amplitude-modulated by an electrooptical modulator. The modulation frequency (40 MHz) corresponded to the 2π -uncertainty range of 3.75m. The modulated beam was focused by a system of lenses, L1, L2, and directed vertically downwards through prisms, P1, P2, and an output mirror, M1.

The return reflected by the sea surface and transmitted through mirrors, M1, M2, was focused by a lens, L3, onto a diaphragm, d1, inserted in the image plane to limit, for the sake of better sensivity, the receiver field of sight. The input aperture, D, was defined by the L3 diameter of 4.7cm, while the d1 diaphragm diameter was from 0.04 to 0.3mm. So the receiver visual angle was $10'$, i.e. the linear dimension of the sea site visible through the diaphragm was from 0.7 to 5cm. The return beam cut-off by the field diaphragm was made to pass through a collimator, L4, and an interference filter, IF, then it was registered by a photomultiplier, PM. The radiopulses of frequency 40 MHz from the PM output were fed to a detector of envelope and phase. The analog envelope and phase signals from the detector were recorded by a Brüel and Kjaer 7005 tape recorder. The signals were also processed using a DISA 56 N11-type mean-value meter, a Brüel and Kjaer 7005 spectrum analyzer, and a CLANP 0270 computer.

The lidar experiments were conducted during May-June 1987 at an oceanographic platform located in the Black Sea 500m off the Crimea coast. Under various hydrometeorological conditions, we carried out 70 series of 20-minute measurements. The distance

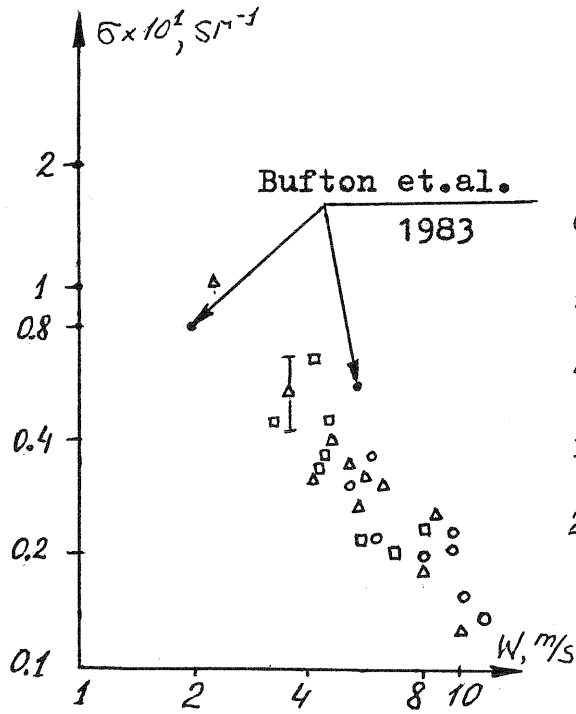


Fig.4 σ versus W .

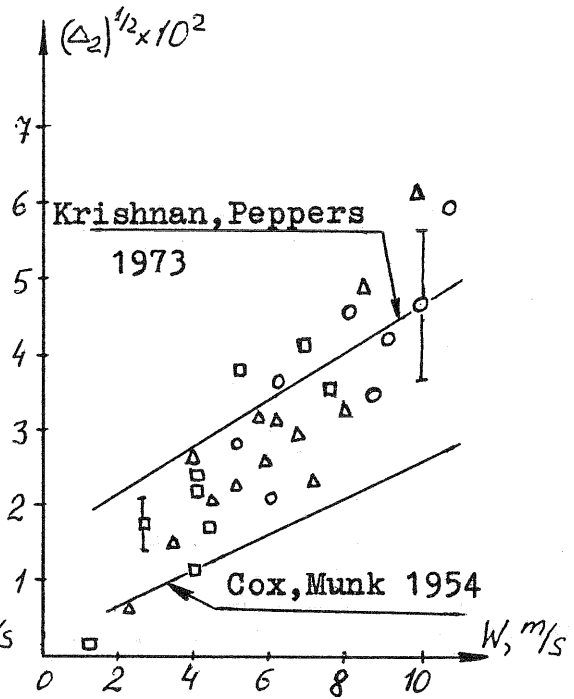


Fig.5 $(\Delta_2)^{1/2}$ versus W .

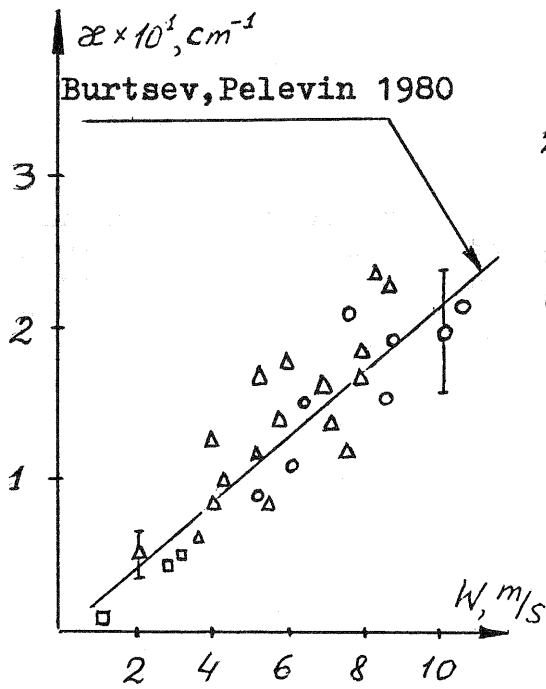


Fig.6 α versus W . $\Delta d=7$
 $\circ d=15$
 $\square d=50$

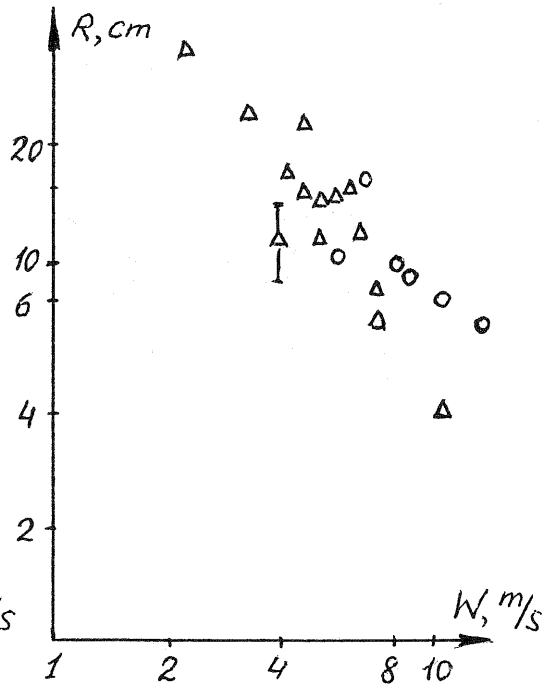


Fig.7 R versus W .

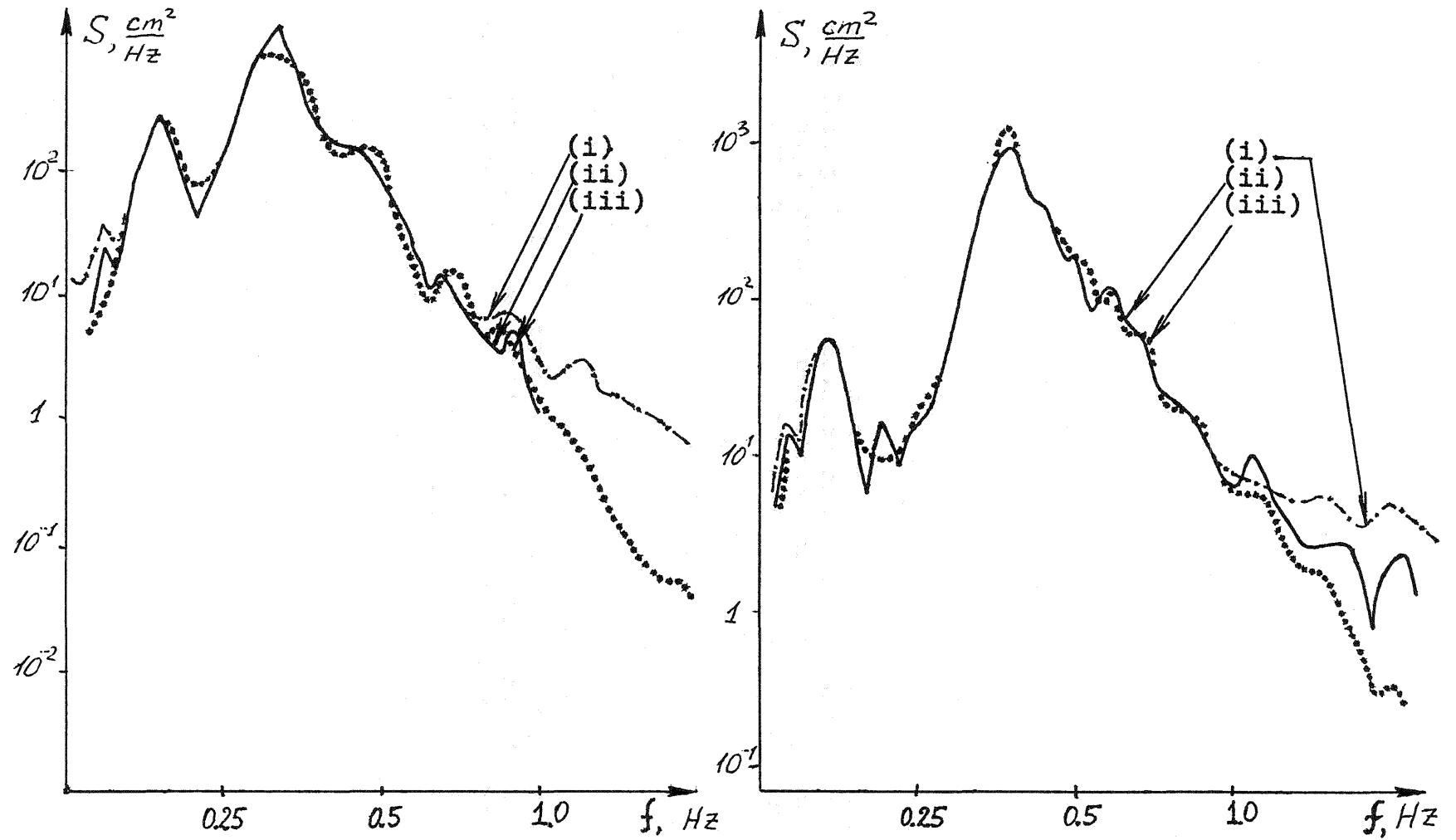


Fig.8 Examples of the spectrum reconstruction.

between the receiving telescope and the sea was 16m. Some of the experimental series were accompanied by in situ measurements with a standard wire waverecorder.

5. DATA ANALYSIS AND DISCUSSION. After processing the return envelope in accordance with (7)-(10), we evaluated $\sigma, \Delta_2 = (\beta_x, \beta_y)^2$, $\kappa = \langle |\Omega| \rangle^{1/2}$, and $R = \langle |\Omega| \rangle^{1/2}$, then analyzed their dependence on the wind velocity, W . Spectral processing of the phase signal and its correction (11) allowed us to determine the sea spectra under various winds. The results were checked partly by wire waverecords and compared to the data reported elsewhere. The sea cross-section versus the wind velocity for different sounding spots is plotted in Fig. 4. The value of σ for vertical incidence falls rapidly with the wind strength and it varies from 0.5 to 0.01, when W changes from 1 to 12 m/s. For comparison, we show here the data [5] obtained with an airborne green (530 nm) pulse Nd:YAG lidar.

Assuming the Gaussian sea statistics, we can readily evaluate the product $\beta_x \beta_y$ of slope variances from σ . Fig. 5 sketches the relationship between $\beta_x \beta_y$ and W , as well as $\Delta^{1/2}(W)$, which is derived from semiempirical [11] relations $\beta_x^2(W)$, $\beta_y^2(W)$ and evaluated from a model [12] spectrum. As seen, our data are in a satisfactory agreement with the results cited. Figs. 6, 7 show the experimental graphs $\kappa(W)$ and $R(W)$, respectively. Fig. 6 also gives the semiempirical [13] relationship $\kappa(W)$. The errors present in Figs. 4 through 7 are related to the imperfect lidar graduation. The variations in experimental data may be partly attributed to several uncontrollable factors, i.e. to duration and length of wind fetch, wind turbidity, differing temperatures of the air and sea, etc. Notice also that, at the widest sounding spot of 5 cm dia, correct measurements of κ and R are possible only under rather slight ($W < 4\text{m/s}$) winds because under stronger winds the specular point density increases sharply and the condition (v) of narrow spot (Sect. 2) is no longer fulfilled. Figs. 8a, b exemplify different sea spectra, where we demonstrate: (i) the spectrum of an initial phase signal; (ii) the phase spectrum corrected in accordance with (11); and (iii) the waverecorder surface elevation spectra; respectively. A comparison of all the spectra exhibits good coincidence of the rough lidar and recorder data up to frequency of 1,25 Hz. After correction the upper limit of the coincidence shifts to around 2.5 Hz.

Thus, the suggested method enables a noticeable progress to be made in lidar remote measurements of the high-frequency sea waves and of the slope variance and the curvature of a disturbed sea.

REFERENCES

1. Vesecky J.F. and Stewart R.M. The observation of ocean surface phenomena, using imagery from the SEASAT synthetic aperture radar: An assessment. J. Geophys. Res. C87, 3397-3430, 1982.
2. Alpers W.R., Ross D.B. and Rufenach C.L. On the detectability

- of ocean surface waves by real and synthetic aperture radar. J. Geophys. Res. C86, 6481-6498, 1981.
3. Skolnik M., Ed. Radar Handbook. McGraw-Hill, N.Y., 1970.
 4. Prokhorov A.M., Ed. Laser Handbook. Sovradio, Moscow, 1978.
 5. Bufton J.L., Hoge F.E. and Swift R.N. Airborne measurements of laser backscatter from the ocean surface. Appl. Opt. 22, 2603-2618, 1983.
 6. Barrick D.E. Relationship between slope probability density function and the physical optics integral in rough surface scattering. Proc. IEEE 56, 1728-1729, 1968.
 7. Tsai B.M. and Gardner C.S. Remote sensing of sea state using laser altimeters. Appl. Opt. 21, 3932-3940.
 8. McClain C.R., Chen D.T. and Hart W.D. On the use of laser profilometry for ocean wave studies. J. Geophys. Res. C87, 9509-9515, 1982.
 9. Bunkin F.V.; Voliak K.I., Malyarovskiy A.I., Mikhalevich V.G., Solntsev M.V., Shevchenko T.B. and Shugan I.V. Measuring sea waves by reflected laser emission statistics. In: Oceanic Remote Sensing. Nova Sci. N.Y., 3-22, 1987.
 10. Boyer L. and Scarby G. Random sampling: Distortion and reconstruction of velocity spectra from fast Fourier-transform analysis of the analog signal of a laser Doppler processor. J. Appl. Phys. 60, 2699-2707, 1986.
 11. Cox C.S. and Munk W.H. Statistics of the sea surface derived from sun glitter. J. Marine Res. 13, 198-227, 1954.
 12. Krishan K.S. and Peppers N.A. Scattering of Laser Radiation from the Ocean Surface. Stanford Research Inst., Menlo Park, Calif., Final Rep. ONR Contract N0014-73-c-0445, 1973.
 13. Burtsev Ju.S. and Pelevin V.N. Distribution of reflecting facets of waving sea surface on their curvature. In: Light Fields in the Ocean, IOAN, Moscow, 231-232, 1980.